Chen *et al. Zoonoses* (2023) 3:44
DOI 10.15212/ZOONOSES-2023-0013

ORIGINAL ARTICLE

NA_{N342K} Mutation Enhances the Pathogenicity of Influenza B Virus in Mice

Qi Chen[1,2], Xiaohao Xu[1,2], Min Tan[2], Lei Yang[2], Dayan Wang[2], Yuelong Shu[1,3,*] and Wenfei Zhu[2,*]

Abstract

Objective: Influenza B virus is a significant respiratory pathogen responsible for seasonal influenza. In recent years the B/Yamagata lineage has demonstrated a rapid increase, predominantly featuring the neuraminidase $(NA)_{N342K}$ mutation. This study determined the impact of the NA_{N342K} mutation on the pathogenicity of influenza B virus and elucidate the underlying mechanisms.

Methods: Gene fragments with specific mutations were generated using site-directed mutagenesis PCR, resulting in recombinant viruses (rAH127 and rAH127/NA_{N342K}). C57BL/6 mice were infected to evaluate the impact of amino acid mutations on virus pathogenicity. Body weight, survival rate, virus replication, and lung pathology were compared among the groups. NA enzyme activity was assessed to determine the mechanisms underlying the effects of amino acid mutations on the pathogenicity of influenza B virus.

Results: The NA_{N342K} mutant virus exhibited significantly increased NA enzyme activity (3.19-fold) and viral replication capacity in MDCK cells (6.76-fold) compared to wild-type virus. These changes led to enhanced pathogenicity in mice, characterized by severe weight loss, increased mortality, and heightened lung tissue inflammation.

Conclusions: The NA_{N342K} mutation likely enhances virus replication and pathogenicity by increasing NA enzyme activity. These findings contribute to understanding the molecular mechanisms underlying influenza B virus pathogenicity and have implications for targeted therapeutic strategies.

Key words: influenza B virus, epidemiology, pathogenicity, neuraminidase

***Corresponding authors:**
E-mail: shuylong@mail.sysu.edu.cn, Tel: +86-10-80829508 (YS); wenfei@cnic.org.cn, Tel: +86-10-58900854 (WZ)

[1]School of Public Health (Shenzhen), Shenzhen Campus, Sun Yat-sen University, Shenzhen 518107, P.R. China
[2]National Institute for Viral Disease Control and Prevention, Chinese Centers for Disease Control and Prevention; Key Laboratory for Medical Virology, National Health Commission, Beijing 102206, P.R. China
[3]Institute of Pathogen Biology, Chinese Academy of Medical Sciences & Peking Union Medical College, Beijing 102629, P.R.China

Received: April 12 2023
Revised: July 6 2023
Accepted: September 1 2023
Published Online: November 11 2023

INTRODUCTION

Seasonal influenza is an acute respiratory infection caused by influenza viruses that has a significant burden on the global healthcare system and can lead to severe complications, including death [1]. The viruses that cause seasonal influenza are influenza A virus (IAV) and influenza B virus (IBV). IAV accounts for the majority of cases, while IBV accounts for approximately 20%–30% of cases [2,3]. From 2000–2018 in 31 countries around the world, there were 118 and 125 influenza seasons during which the proportion of IBV cases was < 20% and 20%–50%, respectively. Moreover, IBV was responsible for > 50% of cases in 45 influenza seasons. Notably, approximately one in seven influenza seasons was predominantly characterized by IBV [4]. From 2003–2008 IBV was responsible for

> 50% of the influenza-related deaths and the excess mortality associated with IBV-dominated seasons surpassed that observed in H3N2- or H1N1-dominated seasons [5]. IBV may cause more severe disease than IAV in children. Retrospective data from 12 Canadian pediatric hospitals from 2004–2013 showed that hospitalized patients (age ≤16 years) infected with IBV had a higher mortality rate than IAV. Healthy children ≥ 10 years of age had a significantly increased risk of ICU admission for IBV infection [6,7]. Therefore, the threat of IBV should not be underestimated.

The first strain of IBV was successfully isolated in 1940. Since the 1980s, IBV has gradually evolved into two antigenically distinct phylogenetic lineages (B/Victoria and B/Yamagata), which have co-circulated globally [8-10]. The B/Yamagata virus diverged before 2000, leading to long-term co-circulation of two different antigenic branches with an alternating antigenic dominance epidemic pattern between seasons [11,12]. During the last decade, the hemagglutinin (HA) and neuraminidase (NA) antigens of B/Yamagata viruses have drifted more rapidly than observed in previous decades, surpassing the drift behavior of B/Victoria lineage viruses.

During the evolutionary process, the amino acid at the NA342 site had a mutation from D-to-N around 2014; after 2016, a mutation from N-to-K emerged. We have previously reported that the 342 site is close to the enzyme active site in the spatial structure of NA, and the N342D mutation significantly increases NA enzyme activity and increases the pathogenicity of the virus [13]. Whether the amino acid mutation from N-to-K will affect the pathogenicity of the virus has not been fully studied. Therefore, in this study we generated virus containing N-to-K mutations using reverse genetics techniques and investigated the effect of such mutations on viral pathogenicity and the possible underlying mechanisms.

MATERIALS AND METHODS

Data sources

The NA fragment sequences of B/Yamagata influenza virus, which were isolated in China from 2011–2019 were downloaded from the Global Initiative on Sharing All Influenza Data (GISAID). The influenza etiology detection data came from the influenza epidemic prediction and early warning platform of the Chinese National Influenza Center (CNIC). Sequence alignment was performed using MAFFT (v7.505) and the results were exported using MEGA 7.0 software.

Cell culture

Madin-Darby canine kidney (MDCK) and human embryonic kidney (293T) cells were grown and maintained in Dulbecco's modified Eagle's medium (DMEM; Invitrogen, Carlsbad, California, U.S.) supplemented with 10% fetal bovine serum (FBS; Invitrogen), HEPES (10 mM; Invitrogen), penicillin (100 units/ml; Invitrogen), and streptomycin (100 μg/ml; Invitrogen). Cells were incubated in a 5% CO_2 humidified atmosphere at 37°C.

Site-directed mutagenesis and virus preparation

All eight gene fragments cloned into a bidirectional pHW2000 vector of B/Anhui-Baohe/127/2015 (AH127/15) were stored in CNIC. Mutations were introduced into the NA gene to generate corresponding mutant fragments. As previously stated, eight reverse genetic plasmids bearing the cDNA of each gene segment were co-transfected into 293T/MDCK cells for 24 h to generate recombinant IBV (SuperFect Transfection Reagent, QIAGEN). The virus was propagated in MDCK cells for 72 h at 33°C using the culture supernatant [14,15]. To verify that no undesired changes were present, all recombinant viruses were thoroughly sequenced. All experiments involving live influenza viruses were carried out in a biosafety level 2 laboratory.

Growth kinetics

MDCK cells were infected with viruses at a multiplicity of infection (MOI) of 0.001. Following a 1-h incubation period at 35°C, the cells were washed twice with phosphate-buffered saline (PBS, HyClone, U.S.). Thereafter, the cells were treated with infection medium containing TPCK-trypsin (sigma-aldrich) at a concentration of 2 μg/mL and incubated at 35°C in 5% CO_2. Cell supernatants were collected at 0, 24, 48, 72, and 96 h post-infection (h.p.i.). The viral titer was determined by evaluating the tissue culture infectious dose ($TCID_{50}$) in MDCK cells.

Pathogenicity experiments in mice

Murine experiments were conducted under the approval of the Ethics Committee of the National Institute for Viral Disease Control and Prevention of the China Centers for Disease Control (20191106040). All studies were conducted using female C57BL/6 mice that were 8 weeks old and specific pathogen-free. The mice were purchased from the SPF (Beijing) Biotechnology Co., Ltd. (Beijing, China). Five mice per group were infected intranasally with PBS or 1×10^1, 1×10^2, 1×10^3, 1×10^4, 1×10^5, 1×10^6, or 1×10^7 $TCID_{50}$ (50 μl) of virus while under isoflurane anesthesia. For a period of 14 days, the body weights and survival of the mice were recorded daily. Mice that lost > 25% of their body weight were humanely euthanized. Serum samples were obtained from living mice 14 days post-infection (d.p.i.) to estimate the 50% mouse infectious dose (MID_{50}). The serum sample hemagglutinin inhibition (HI) antibody titers were determined in 0.5% (vol/vol) turkey red blood cells following treatment with receptor-destroying enzyme (Denka Seiken, Tokyo, Japan) at 37°C for 18 h and inactivation at 56°C for 30 min. HI antibody titers > 10 were regarded as antibody-positive. The MID_{50} and 50% median lethal dose (MLD_{50}) were calculated according to the Karber calculation method [16]. Six mice from each group were given an intranasal injection of 1×10^7 $TCID_{50}$ (50 μl)

virus for the purpose of assessing virus pathogenicity, 3 of which were euthanized at 1 d.p.i. and 3 of which were euthanized at 4 d.p.i. The nostrils and lungs were resected and the $TCID_{50}$ method was used to measure the virus titers in MDCK cells. The right lung lobe of each mouse was preserved in 10% formalin, embedded in paraffin wax, and cut into 4-μm thick slices. Hematoxylin and eosin (HE) were used to stain a single slice of each sample.

NA enzyme activity assay

Neuraminidase activity was assessed using the NA-Fluor™ Influenza Neuraminidase Assay Kit (Invitrogen, Carlsbad, California, U.S.). The virus was diluted 2-fold from 1×10^5 $TCID_{50}$/50 μl-to-1×10^2 $TCID_{50}$/50 μl. Fifty microliters of 200 μM NA-Fluor™ working solution was added to 50 μl of virus solution in each well of a black 96-well plate and incubated at 37°C for 1 h. The reaction was then terminated by adding 100 μl of NA-Fluor™ termination solution, and fluorescence was measured using excitation and emission wavelengths at 365 and 450 nm, respectively. The virus at each titer were determined three times and a PBS blank control was set at the same time.

Statistical analysis

Data are presented as the mean ± SEM. Statistical significance was evaluated using Student's t-test. A P value < 0.05 indicated statistical significance. GraphPad Prism 9 software (GraphPad Software Inc., California, U.S.) was used to generate the figures.

RESULTS

Circulation of IBV between 2012 and 2019 in China

To gain insight into the domestic epidemiology of IBV in China, we performed an analysis of pathogenic surveillance data involving influenza viruses within the country. Before 2012, influenza virus etiologic surveillance did not involve further lineage distinction for positive IBV-positive samples. Therefore, data prior to 2012 were excluded and our analysis focused on the period from 2012–2019. During this timeframe, IAV always accounted for a large proportion of influenza virus-positive samples. Since 2014 the amount and proportion of IBV have increased from 25%-to-> 35%. Viruses of both lineages were detected every year, among which the B/Victoria lineage dominated in 2016 and 2019, accounting for 27.16% and 30.46%, respectively. IBV circulating in the remainder of the year was dominated by the B/Yamagata strain, and the proportion of positive samples in 2015, 2017, and 2018 was > 24% (Fig 1A and B). According to the etiologic surveillance findings, the B/Yamagata lineage among IBV prevailed in China from 2012–2019.

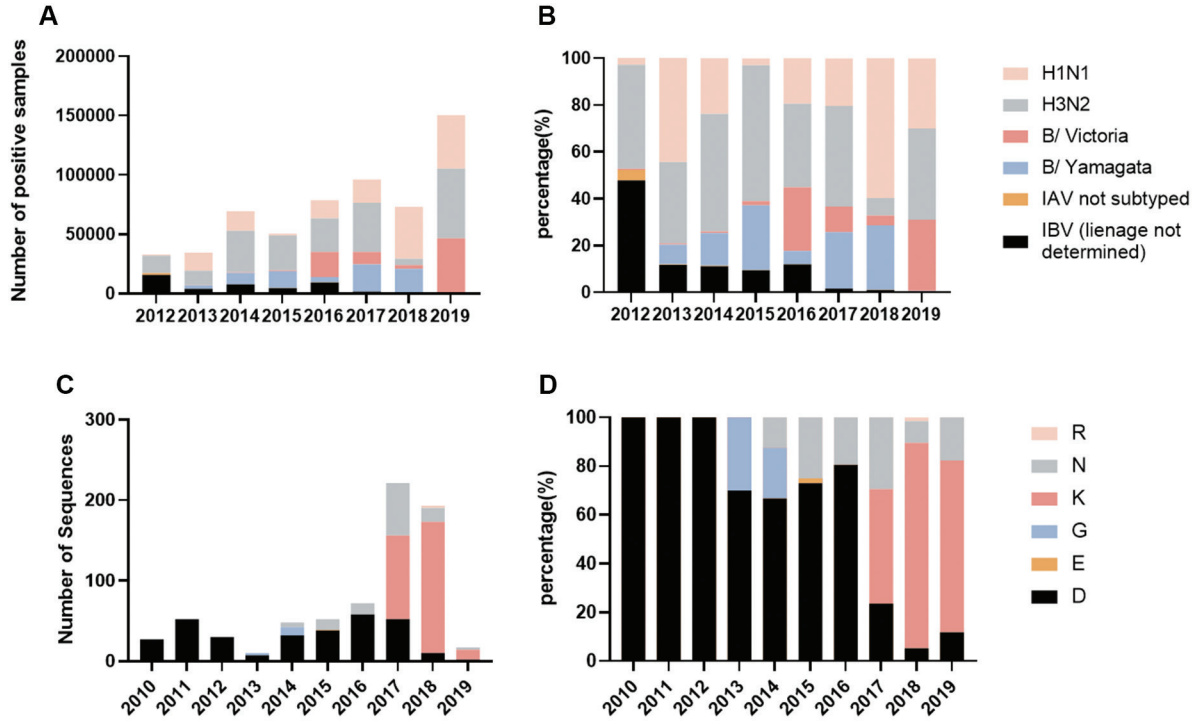

FIGURE 1 | Etiologic surveillance results of influenza viruses in China from 2012–2019.
A: The number of influenza types detected under etiologic surveillance from 2012–2019. B: Proportion of positive results of etiological surveillance for each type of influenza from 2012–2019. C: Sequence numbers of various amino acids appearing at the NA 342 position. Amino acid changes at NA 342 of the B/Yamagata virus from 2010–2019. A total of 723 complete NA sequences of the B/Yamagata virus isolated from China during 2010-2019 were downloaded from the GISIAD official website. After sequence alignment using MAFFT software, amino acids at site 342 in all sequences were statistically analyzed. D: Proportion of various amino acids occurring at the NA 342 position.

Amino acid variations at the 342 position in IBV NA protein

To gain insight into the amino acid variations at residue 342 of the IBV NA protein in China, a total of 723 complete B/Yamagata virus NA sequences from 2010–2019 were downloaded from GISIAD. After sequence alignment, amino acids at site 342 of all sequences were statistically analyzed. As shown in Fig 1C and 1D, a total of 6 kinds of amino acids were found at this site during these 10 years, including D, N, K, R, G, and E. Before 2012, only amino acid D was at this site. After 2013, strains with N mutations at site 342 appeared and continued to exist. Since 2016 strains with the K mutation appeared and the proportion increased rapidly, exceeding the proportion of N and D strains at site 342, thus occupying a dominant position in B/Yamagata virus. Strains containing the G mutation dominated in 2013 and 2014, and strains containing the E and R mutations dominated in 2015 and 2018, respectively.

Effects of the NA_{N342K} mutation on the pathogenicity of IBV in mice

To determine the impact of the NA_{N342K} mutation on the pathogenicity of IBV, recombinant viruses were generated. The 8-plasmid recombinant virus containing wild-type AH127/15 virus was designated rAH127, and the virus with the NA_{N342K} mutation was designated rAH127/NA_{N342K}. Five 8-week-old female C57BL/6 mice were infected with 1×10^1–$1 \times 10^7 TCID_{50}$ of rAH127 or rAH127/NA_{N342K} virus, or PBS. As shown in Fig 2, rAH127/NA_{N342K} virus caused more severe weight loss and a higher mortality rate. Mice infected with $\leq 1 \times 10^6 TCID_{50}$ of the two strains of

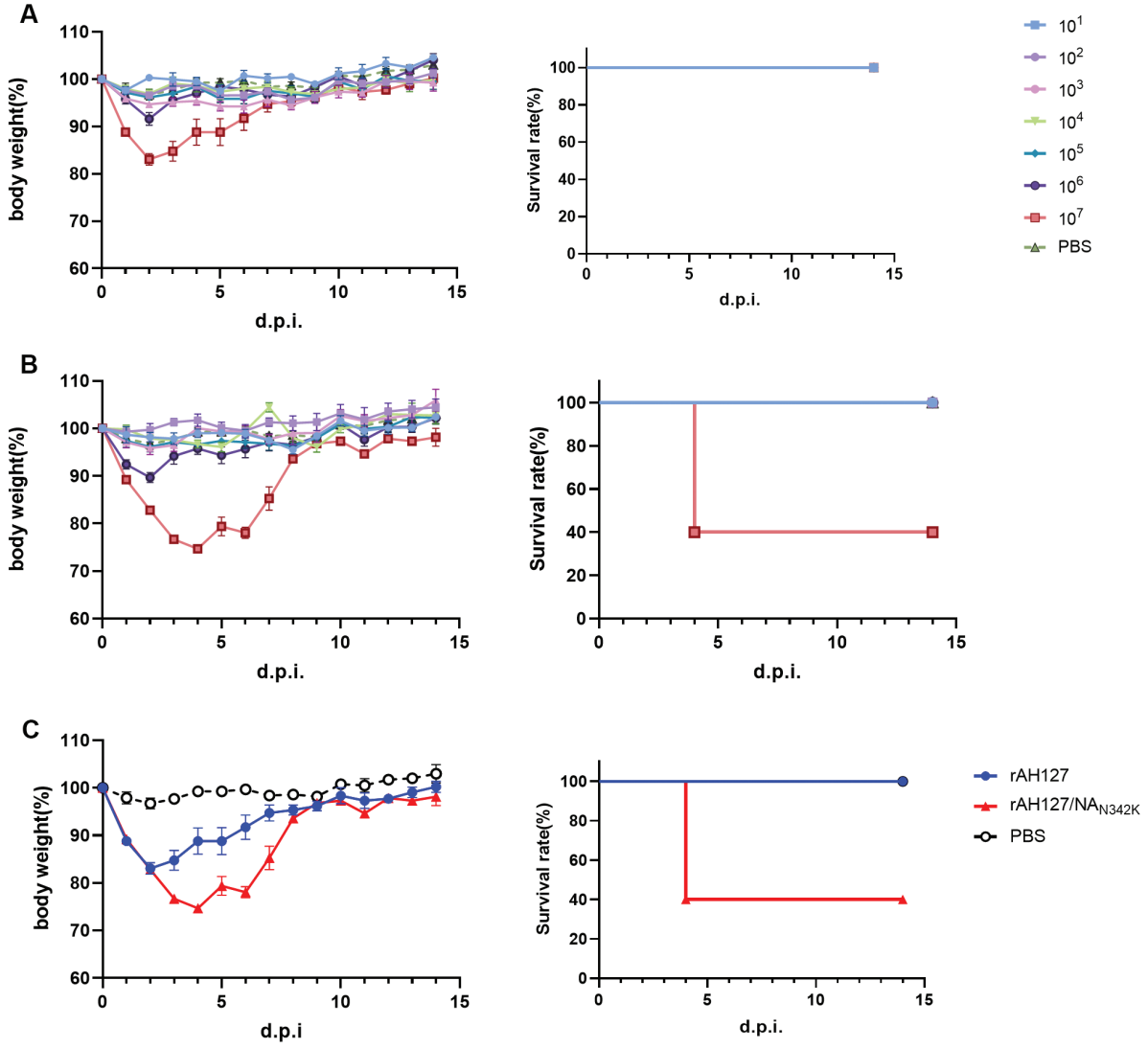

FIGURE 2 | Body weight loss and the survival rate of mice infected with different doses of rAH127 and rAH127/NA_{N342K}. Five mice per group were inoculated intranasally with 10^1–10^7 $TCID_{50}$ titers of rAH127 (A) or rAH127/NA_{N342K} (B) or PBS as a control. Body weight changes (left) and the survival rate (right) were monitored daily. C: Changes in body weight (left) and survival rate (right) in the $10^7 TCID_{50}$ rAH127 and rAH127/NA_{N342K} groups.

virus did not have significant weight loss and recovered quickly after the weight loss. In the rAH127 10^7TCID$_{50}$ group, the mice demonstrated a decline in body weight, reaching a minimum of 82.8% of their original body weight on 2 d.p.i., with gradual recovery observed from 3 d.p.i. onwards. Conversely, in the rAH127/NA_{N342K} group, the body weight nadir was reached on 4 d.p.i. On this same day, three mice succumbed to infection, while the remaining two mice exhibited a gradual recovery in body weight (Fig 2C). According to the HI test, the MID_{50} of both virus strains was not significantly altered (Table 1). The histopathologic examination using HE staining demonstrated that mice infected with rAH127 exhibited mild inflammation on 1 and 4 d.p.i. In contrast, mice infected with rAH127/NA_{N342K} displayed pronounced bronchopneumonic inflammation characterized by substantial infiltration of inflammatory cells surrounding the bronchi and alveoli. Notably, no pathologic alterations were observed in the lungs of mice in the PBS control group (Fig 3). These findings provide evidence that the NA_{N342K} mutation enhanced the inflammatory response in IBV-infected mice.

NA_{N342K} increased viral replication *in vitro*

To determine the replication ability of the two viruses *in vitro*, MDCK cells were infected with viruses and growth kinetics analysis was performed; the results are shown in Fig 4A. At 24 h post-infection, both strains demonstrated effective replication, reaching titers of approximately 4 logTCID$_{50}$/ml. Subsequently, at 48 h post-infection, the replication titers of both strains continued to rise, with rAH127 and rAH127/NA_{N342K} reaching peak titers. The titer of rAH127/NA_{N342K} and rAH127 was 6.94 logTCID$_{50}$/ml and 6.11 logTCID$_{50}$/ml, respectively, and the titer of rAH127/NA_{N342K} was 6.76 times that of rAH127 ($P<0.01$). By 72 h post-infection, the titer of rAH127 remained stable, while the titer of rAH127/NA_{N342K} decreased and was comparable to rAH127. Taken together, these data indicate that the NA_{N342K} mutation enhances the viral replication capacity in MDCK cells.

Effects of NA_{N342K} mutation on enzyme activity

Previous studies have demonstrated that the NA 342 site in IBV is in close proximity to the enzyme active sites (274 and 294), and the N342D mutation significantly enhances IBV NA enzyme activity [9]. To determine the effect of the N342K site on enzyme activity, rAH127 and rAH127/NA_{N342K} NA enzyme activity was measured. The results were quantified as the half-maximal effective concentration (EC_{50}) of the fifth decomposition of the virus. As depicted in Fig 4B, the rAH127/NA_{N342K} NA enzyme activity was approximately 3.19 times higher than rAH127. These findings provide evidence that the N342K mutation augmented IBV NA activity.

TABLE 1 | Hemagglutinin inhibition antibody test of the C57BL/6 mice inoculated with rAH127 and rAH127/NA_{N342K}.

Virus	Inoculation dose (log10 TCID$_{50}$)	HI titer					MID_{50}(log10 TCID$_{50}$)
		#1	#2	#3	#4	#5	
rAH127	7	160	160	160	320	160	1.3
	6	160	80	80	160	80	
	5	160	160	160	160	160	
	4	160	160	80	80	160	
	3	80	40	40	40	40	
	2	40	80	160	20	80	
	1	<10	<10	<10	<10	10	
rAH127/NA_{N342K}	7	320	160	ND	ND	ND	1.1
	6	160	80	320	160	320	
	5	80	160	160	80	80	
	4	80	160	80	80	160	
	3	40	80	40	40	80	
	2	40	20	80	40	10	
	1	40	80	<10	<10	<10	
PBS		<10	<10	<10	<10	<10	

Notes: (1) Sera were collected from each surviving mouse (#1–#5) at 14 d.p.i. and were tested for HI titers against rAH127. The MID_{50} was determined using the Karber method.
(2) ND: Not determined due to death (treated as positive for determination of the MID_{50}). An HI titer < 10 was regarded as negative for seroconversion.

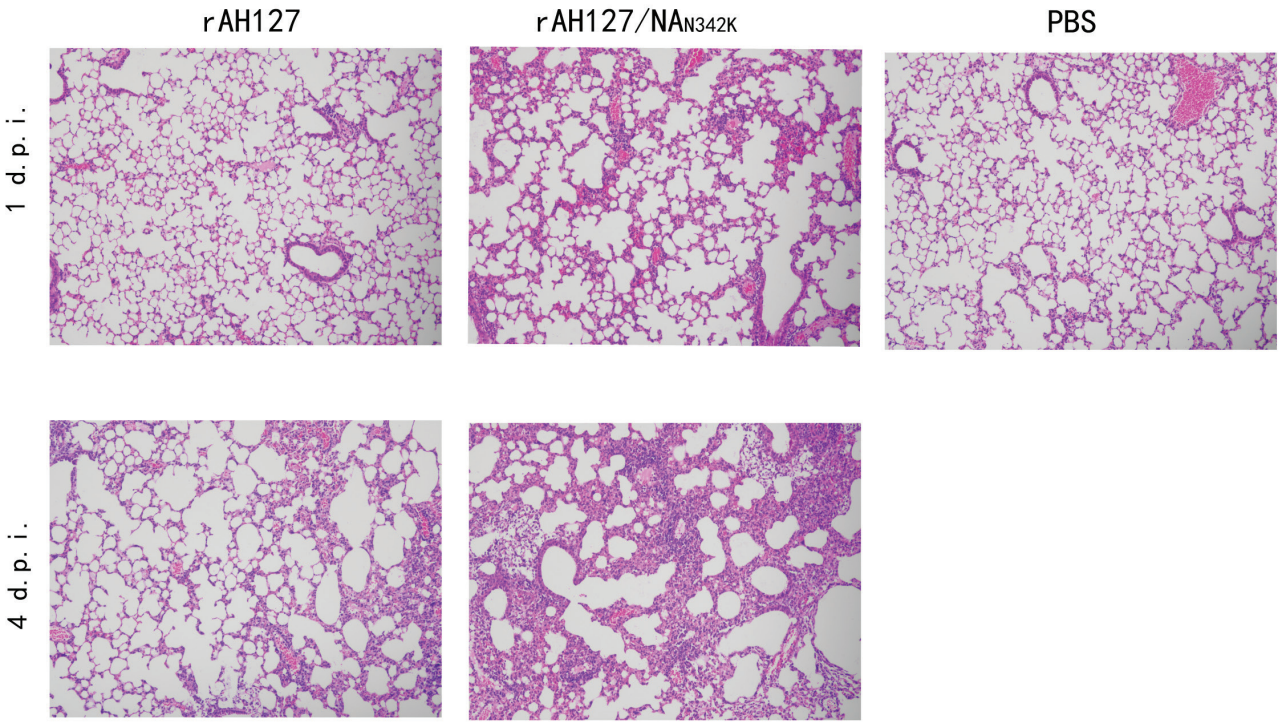

FIGURE 3 | Pathologic changes of lung tissues from mice after virus infection (x100).
Mice were inoculated intranasally with 50 μL 10^7 $TCID_{50}$ of rAH127 or rAH127/NA_{N342K}, or 50 μL of PBS. The right upper lobe of the mouse lung was resected, fixed, stained, observed, and photographed under a 100-fold field of view.

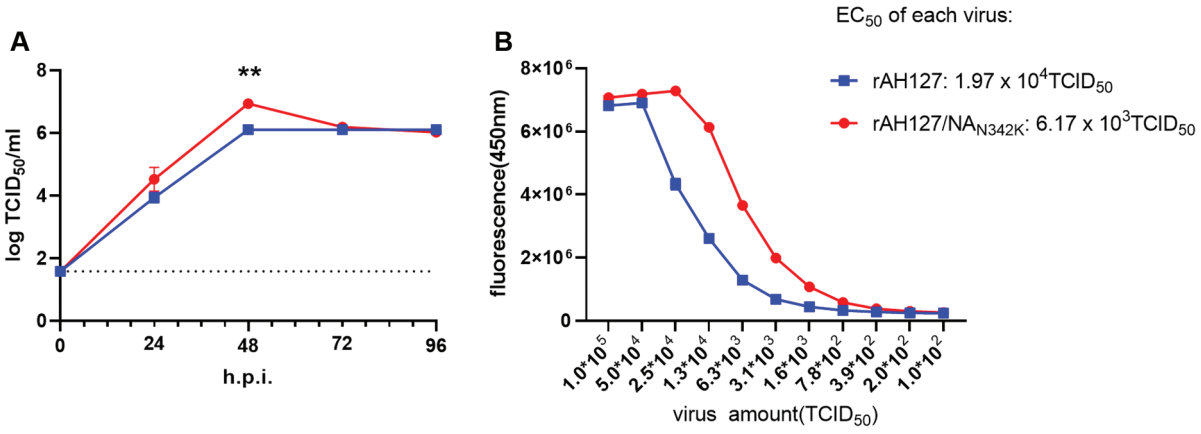

FIGURE 4 | Growth kinetics of rAH127 and rAH127/NA_{N342K} in MDCK cells and NA enzyme activity.
A: MDCK cells were infected with rAH127 and rAH127/NA_{N342K} at 35°C with a MOI of 0.001. The cell supernatants were collected at 0, 24, 48, 72, and 96 h post-infection (h.p.i.). The viral titer was determined by measuring the $TCID_{50}$ in MDCK cells (**P<0.01). B: NA enzyme activities of rAH127 and rAH127/NA_{N342K}.

DISCUSSION

IBV, which was previously thought to be less harmful than IAV due to its limited infectivity to humans, has been shown through numerous clinical studies to have a health impact in humans comparable to IAV. The clinical symptoms associated with both influenza types are similar, as are hospitalization and mortality rates in the general population [17,18]. Surprisingly, IBV has been shown to cause even higher excess mortality in children compared to IAV in some cases [19].

This study focused on the emergence of the B/Yamagata strains and demonstrated a rapid increase in the proportion of strains containing the NA_{N342K} mutation. Furthermore, it was shown that the virus carrying this mutation exhibited heightened pathogenicity in mice, resulting in increased

weight loss, a higher mortality rate, and more severe pulmonary inflammatory lesions (Figs 2 and 3).The enzyme activity of rAH127/NA_{N342K} is 3 times higher than rAH127. Based on these findings, we offer the hypothesis that the mutation enhances the pathogenicity of the virus by increasing NA enzyme activity.

NA is a tetramer composed of four identical peptides and accounts for 10%–20% of the total glycoprotein on the surface of influenza viruses [20]. The primary function of NA involves catalyzing the attachment between the sialic acid receptor and HA during the late stage of viral replication, facilitating the release of newly synthesized progeny virions from the host cell surface [21-23]. Additionally, NA has been shown to play a role in the cellular entry of the virus and enhance infection efficiency [24]. Zhang et al. [25] reported that the NA_{D272N} mutation in H5N6 significantly increased replication and virulence in mice. Compared with amino acids N272 and S272, the NA protein of amino acid D272 may be structurally unstable [25]. The NA active site is comprised of an inner layer of 8 highly conserved residues that directly interact with sialic acid, and an outer layer of 10 residues that do not come into contact with sialic acid, but possess crucial structural functions [20].

In a previous study it was shown that the spatial location of the NA_{N342D} mutation was close to the enzymatic active sites mentioned above, which could increase the MLD_{50} of the virus by > 10-fold and the NA enzyme activity by 20-fold, greatly increasing the pathogenicity of the virus. Similarly, the N342K mutation also heightened virus pathogenicity, albeit to a lesser extent compared to the N342D mutation and resulted in a less pronounced increase in NA enzyme activity. Following the emergence of the N342K mutation, however, the prevalence of viruses containing either N or D decreased rapidly, particularly in 2017 and 2018. IBVs accounted for approximately 30% of pathogen surveillance, with a majority being B/Yamagata viruses harboring the NA_{N342K} mutation. This observation led us to speculate that viruses carrying the NA_{N342K} mutation might exhibit higher transmissibility. Nevertheless, the precise transmission capacity and underlying mechanisms necessitate further investigation. According to the influenza surveillance results of the WHO, IBV was at a low epidemic level in a short period of time after 2020 due to the impact of COVID-19, but in the 2021-2022 influenza season IBV re-circulation in China caused a large number of influenza outbreaks [26], suggesting that we should strengthen surveillance of IBV.

In summary, we identified a novel molecular marker (the NA_{N342K} mutation) that enhances the pathogenicity of IBV, thus providing new insights for IVB research and surveillance in the future.

ACKNOWLEDGEMENTS

This study was supported by the National Nature Science Foundation of China (81971941) and the National Key Research and Development Program of China (2022YFC2303801 and 2021YFC2300100). The opinions expressed by the authors contributing to this journal do not necessarily reflect the opinions of the Centers for Disease Control and Prevention or the institutions with which the authors are affiliated.

CONFLICTS OF INTEREST

Yuelong Shu is Deptuy Editor-in-Chief of *Zoonoses*. Dayan Wang is a member of Editorial Board of *Zoonoses*. Neither Yuelong Shu nor Dayan Wang is involved in the peer review or decision-making process of the manuscript. The other authors have no competing interests to disclose.

REFERENCES

1. Belazi S, Olsen SJ, Brown C, Green HK, Mook P, Nguyen-Van-Tam J, et al. Spotlight influenza: Laboratory-confirmed seasonal influenza in people with acute respiratory illness: a literature review and meta-analysis, WHO European Region, 2004 to 2017. Euro Surveill. 2021;26(39):2000343.
2. Paul Glezen W, Schmier JK, Kuehn CM, Ryan KJ, Oxford J. The burden of influenza B: a structured literature review. Am J Public Health. 2013;103(3):e43-e51.
3. Zaraket H, Hurt AC, Clinch B, Barr I, Lee N. Burden of influenza B virus infection and considerations for clinical management. Antiviral Res. 2021;185:104970.
4. Caini S, Kusznierz G, Garate VV, Wangchuk S, Thapa B, de Paula Júnior FJ, et al. The epidemiological signature of influenza B virus and its B/Victoria and B/Yamagata lineages in the 21st century. PLoS One. 2019;14(9):e0222381.
5. Feng L, Shay DK, Jiang Y, Zhou H, Chen X, Zheng Y, et al. Influenza-associated mortality in temperate and subtropical Chinese cities, 2003-2008. Bull World Health Organ. 2012;90(4):279-288B.
6. Tran D, Vaudry W, Moore D, Bettinger JA, Halperin SA, Scheifele DW, et al. Hospitalization for influenza A versus B. Pediatrics. 2016;138(3):e20154643.
7. Taniguchi K, Ikeda S, Hagiwara Y, Tsuzuki D, Klai M, Sakai Y, et al. Epidemiology and burden of illness of seasonal influenza among the elderly in Japan: a systematic literature review and vaccine effectiveness meta-analysis. Influenza Other Respir Viruses. 2021;15(2):293-314.
8. Vijaykrishna D, Holmes EC, Joseph U, Fourment M, Su YC, Halpin R, et al. The contrasting phylodynamics of human influenza B viruses. Elife. 2015;4:e05055.
9. Rota PA, Wallis TR, Harmon MW, Rota JS, Kendal AP, Nerome K. Cocirculation of two distinct evolutionary lineages of influenza type B virus since 1983. Virology. 1990;175(1):59-68.
10. Puzelli S, Di Martino A, Facchini M, Fabiani C, Calzoletti L, Di Mario G, et al. Co-circulation of the two influenza B lineages during 13 consecutive influenza surveillance seasons in Italy, 2004-2017.BMC Infect Dis. 2019;19(1):990.
11. Virk RK, Jayakumar J, Mendenhall IH, Moorthy M, Lam P, Linster M, et al. Divergent evolutionary trajectories of influenza B viruses underlie their contemporaneous epidemic activity. Proc Natl Acad Sci U S A. 2020;117(1):619-628.
12. Langat P, Raghwani J, Dudas G, Bowden TA, Edwards S, Gall A, et al. Genome-wide evolutionary dynamics of influenza B viruses on a global scale. PLoS Pathog. 2017;13(12):e1006749.
13. Zhou L, Feng Z, Liu J, Chen Y, Yang L, Liu S, et al. A single N342D substitution in Influenza B Virus NA protein determines viral pathogenicity in mice. Emerg Microbes Infect. 2020;9(1):1853-1863.
14. Jackson D, Elderfield RA, Barclay WS. Molecular studies of influenza B virus in the reverse genetics era. J Gen Virol. 2011;92(1):1-17.
15. Cardenas-Garcia S, Caceres CJ, Rajao D, Perez DR. Reverse genetics for influenza B viruses and recent advances in vaccine development. Curr Opin Virol. 2020;44:191-202.

16. Ramakrishnan MA. Determination of 50% endpoint titer using a simple formula. World J Virol. 2016;5(2):85-86.
17. Su S, Chaves SS, Perez A, D'Mello T, Kirley PD, Yousey-Hindes K, et al. Comparing clinical characteristics between hospitalized adults with laboratory-confirmed influenza a and B virus infection. Clin Infect Dis. 2014;59(2):252-255.
18. Sočan M, Prosenc K, Učakar V, Berginc N. A comparison of the demographic and clinical characteristics of laboratory-confirmed influenza B Yamagata and Victoria lineage infection. J Clin Virol. 2014;61(1):156-160.
19. van de Sandt CE, Bodewes R, Rimmelzwaan GF, de Vries RD. Influenza B viruses: not to be discounted. Future Microbiol. 2015;10(9):1447-1465.
20. McAuley JL, Gilbertson BP, Trifkovic S, Brown LE, McKimm-Breschkin JL. Influenza virus neuraminidase structure and functions. Front Microbiol. 2019;10:39.
21. Bao D, Xue R, Zhang M, Lu C, Ma T, Ren C, et al. N-linked glycosylation plays an important role in budding of neuraminidase protein and virulence of influenza viruses. J Virol. 2021;95(3):e02042-20.
22. Wen F, Wan XF. Influenza neuraminidase: underrated role in receptor binding. Trends Microbiol. 2019;27(6):477-479.
23. McKimm-Breschkin JL. Influenza neuraminidase inhibitors: antiviral action and mechanisms of resistance. Influenza Other Respir Viruses. 2013;7 (Suppl 1):25-36.
24. Ohuchi M, Asaoka N, Sakai T, Ohuchi R. Roles of neuraminidase in the initial stage of influenza virus infection. Microbes Infect. 2006;8(5):1287-1293.
25. Zhang J, Wang X, Ding S, Ma K, Jiang Y, Guo Y, et al. Key amino acid position 272 in neuraminidase determines the replication and virulence of H5N6 avian influenza virus in mammals. iScience. 2022;25(12):105693.
26. Huang WJ, Cheng YH, Tan MJ, Liu J, Li XY, Zeng XX, et al. Epidemiological and virological surveillance of influenza viruses in China during 2020-2021. Infect Dis Poverty. 2022;11(1):74.